
Controlling the structural and electrical properties of diacid Oligo(Phenylene Ethynylene) Langmuir-Blodgett films

Luz Marina Ballesteros,^[a,b] Santiago Martín,^[c,d] Javier Cortés,^[a,b] Santiago Marqués-González,^[e] Simon J. Higgins,^[f] Richard J. Nichols,^[f] Paul J. Low,^[e] and Pilar Cea^{*,[a,b,d]}

Abstract: This paper describes the preparation, characterization and electrical properties of Langmuir-Blodgett films comprised of a symmetrically substituted oligomeric phenylene ethynylene derivative, namely 4,4'-(1,4-phenylenebis(ethyne-2,1-diyl))dibenzoic acid (OPE2A). Analysis of the surface pressure vs. area per molecule isotherms and Brewster Angle Microscopy reveal that good quality Langmuir (L) films can be formed both onto pure water and a basic subphase. Monolayer Langmuir films were transferred onto solid substrates with a transfer ratio of 1 to obtain Langmuir-Blodgett films (LB). Both L and LB films prepared on or from a pure water subphase show a red-

shift in the UV-vis spectra of ca. 14 nm, in contrast to L and LB films prepared from a basic subphase, which show a hypsochromic shift of 15 nm. This result together with XPS and QCM experiments conclusively demonstrate the formation of one layer LB films in which OPE2A molecules are chemisorbed onto gold substrates and consequently -COO-Au junctions are formed. In LB films prepared on a basic subphase the other terminal acid group is also deprotonated. In contrast, LB films prepared from a pure water subphase preserve the protonated acid group and lateral H-bonds with neighbouring molecules giving rise to a supramolecular structure. STM based conductance studies have revealed that

films prepared from a basic subphase are more conductive than the analogous films prepared on from pure water. Their electrical conductance coincides more closely with the single molecule conductance measurements. This result has been interpreted not only in terms of a better electron transmission in -COO-Au molecular junctions but also in terms of the presence of lateral hydrogen bonds in the films formed from pure water which led to a reduced conductance of the molecular junctions.

Keywords: Langmuir-Blodgett films; oligomeric phenylene ethynylene; STM

Introduction

The development of smaller and more efficient electronic devices has been a perennial concern for researchers and companies in the electronic industry. Since the seminal publication of Aviram and Ratner^[1] molecular electronics has been a much discussed futuristic alternative to present-day silicon based technologies. However, a confounding number of significant challenges need to be addressed before this technology reaches fruition, and practical molecular electronic devices still remain a concept rather than a nascent technology. However, the impact of molecular electronics to understanding charge transport in molecules has been more immediate. In particular, over the last decade it has become clear that the contact between metal and molecule plays a much more determining role on the electronic transmission than was previously envisaged. In this regard much attention has shifted in recent years

to understanding and controlling metal-molecule contacts and developing new surface contacting paradigms.^[2-26] For the development of new devices based on molecular electronics,^[27, 28] it is of crucial importance to be able to understand the chemical nature and structural properties of metal|molecule|metal junctions since the nature of the metal|molecule interface strongly influences the transport properties in molecular devices.^[29] A number of factors, including geometry of contacts,^[30-32] bonding,^[33-35] molecule-electrode distance,^[36-38] or molecular orientation,^[39, 40] have also been found to affect the transport process. Even more, it still remains a challenge to determine experimentally the role of the molecule-metal interface on the transport process, and correlations between experimental observation and theoretical models remain challenging given the size of the computational problem and the variability of individual measurements.^[15, 21, 32, 41-44] In addition, the electron transfer process across the molecule|electrode junction is poorly understood,^[45, 46] and problems related to this topic, such as the structure of the molecule-surface contact, dynamics of electron transfer and the transfer mechanism are topics of ongoing interest. In seeking to address some of these issues, the study of oligophenyleneethynylene (OPE) derivatives, which have shown promising characteristics for their use in molecular electronics, has been proven instructive.^[2, 47-57] Thus, OPEs have been of particular interest in molecular electronics due to their effective π -conjugation and rod-like structure.

Whilst many of these recent studies have been based on single molecule measurements, more closely packed self-assembled (SA) and Langmuir-Blodgett (LB) films have provided important data concerning the electrical properties of monolayer films of active molecular components more likely to find application in device

[a] Departamento de Química Física, Facultad de Ciencias, Universidad de Zaragoza, 50009, Spain.

[b] Instituto de Nanociencia de Aragón (INA), Edificio i+d. Campus Rio Ebro, Universidad de Zaragoza, C/Mariano Esquillor, s/n, 50017 Zaragoza, Spain.

[c] Instituto de Ciencia de Materiales de Aragón (ICMA), Universidad de Zaragoza-CSIC, Departamento de Física de la Materia Condensada, 50009 Zaragoza, Spain

[d] Laboratorio de Microscopías Avanzadas (LMA) C/ Mariano Esquillor s/n Campus Rio Ebro, 50018, Zaragoza, Spain.

[e] Department of Chemistry, University of Durham, Durham DH1 3LE, United Kingdom.

[f] Department of Chemistry, University of Liverpool, Crown Street, Liverpool, L69 7ZD, United Kingdom.

* Corresponding author: pilarcea@unizar.es

architectures. The two main advantages of the LB method over SA films are (i) the compatibility of the LB technique with a wide variety of metal/organic interfaces through the large number of different polar functional groups that can be physically or chemically adsorbed onto an equally wide array of substrates as well as (ii) the fabrication of directionally oriented films containing two different groups that can be chemisorbed onto metal substrates.^[58]

It is the aim of this paper to provide new data about the electrical properties of metal | acid molecular junctions. For a better understanding of the role played by ionic and coordination interactions as well as the influence of the pH on the electrical properties of the films, the molecule 4,4'-(1,4-phenylenebis(ethyne-2,1-diyl))dibenzoic acid, abbreviated as OPE2A, has been synthesized and assembled in LB films (Figure 1), with the films quality being compared to SA films. In addition, the electrical properties of the films prepared under different experimental conditions have been determined and compared with the single molecule conductance.

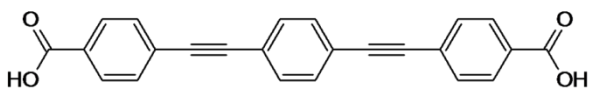


Figure 1. Molecular structure of 4,4'-(1,4-phenylenebis(ethyne-2,1-diyl))dibenzoic acid

Results and Discussion

Fabrication of Langmuir and Langmuir-Blodgett films. The compound OPE2A is characterized by a rigid molecular structure with a highly conjugated π -electron system. In a manner entirely analogous to other amphiphilic molecules containing large polyaromatic moieties, OPE2A has a large tendency to aggregate due to strong π - π interactions,^[59-61] as well as to the facility of acids to aggregate in organic solvents. Thus, the Lambert-Beer law is only followed at concentrations lower than $2.5 \cdot 10^{-5}$ M (Figure 2) in a mixture of chloroform:ethanol 4:1, with higher concentrations leading to deviations from linearity in the absorbance vs. concentration plot. Consequently, highly diluted solutions are required to fabricate true monolayers at the air-water interface. The UV-vis spectrum of this compound in solution features one peak at 328 nm with two shoulders at 359 and 380 nm attributable to π - π^* electronic transitions.^[6, 62]

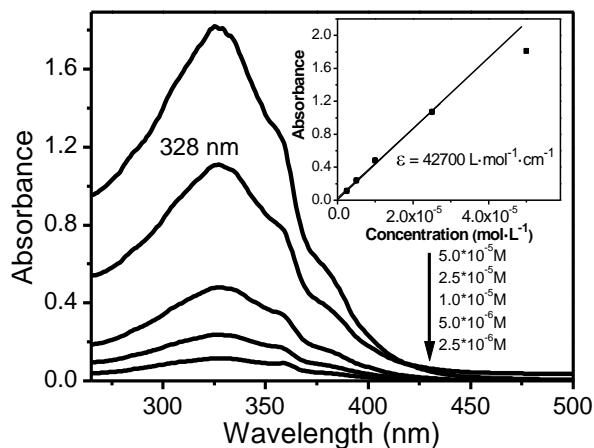


Figure 2. UV-vis spectra of OPE2A in CHCl_3 :EtOH 4:1 solution for the indicated concentrations. Molar absorptivity at 328 nm is $42700 \text{ L}\cdot\text{mol}^{-1}\cdot\text{cm}^{-1}$.

A preliminary investigation of the formation of Langmuir films of OPE2A involving both the concentration and the volume of the spreading solution concluded that only solutions of concentration $1 \cdot 10^{-5}$ M or lower yield reproducible isotherms. Figure 3 shows a representative surface pressure (π -A) isotherm of OPE2A on a water subphase (pH = 5.9) as well as isotherms recorded in a basic subphase (NaOH pH = 11.4). In contrast with other OPE acid derivatives for which a basic subphase was necessary to avoid aggregation,^[19, 26, 63] the Langmuir films of OPE2A were homogeneous (see BAM images in Figure 4) and did not show any evidence of three dimensional (3D) aggregates when a water subphase was used. The π -A isotherms of OPE2A on pure water are characterized by a zero surface pressure, i.e. gas phase, until an area of $0.8 \text{ nm}^2\cdot\text{molecule}^{-1}$ is reached with a gas to an expanded liquid phase transition taking place for the monolayer fabricated onto a water subphase. When the pH increases, the lift-off area per molecule decreases, with a value of $0.6 \text{ nm}^2\cdot\text{molecule}^{-1}$ for the monolayers obtained onto a basic subphase. The lift-off in the isotherms is followed by a monotonous increase of the surface pressure upon compression.

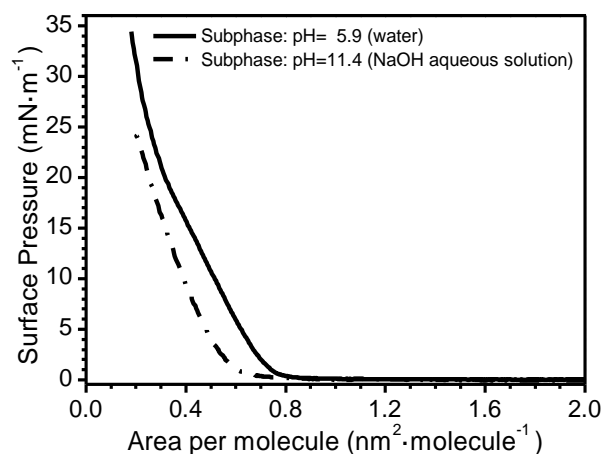


Figure 3. Surface pressure vs. area per molecule isotherm of OPE2A on a water subphase and a NaOH aqueous subphase at 20°C .

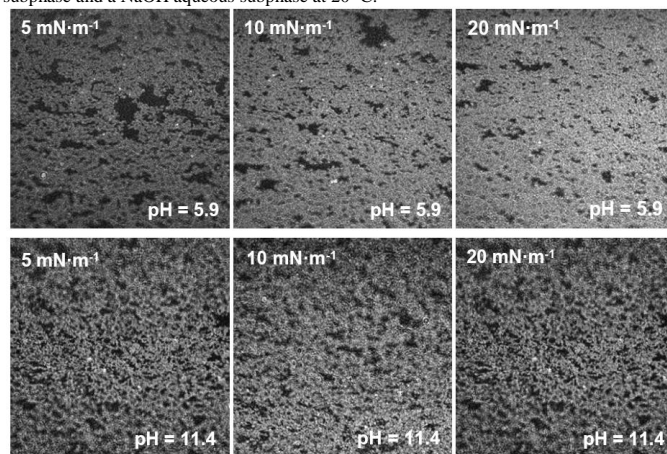


Figure 4. BAM images recorded at the indicated surface pressures for a pure water subphase (pH = 5.9) and a basic subphase (pH=11.4)

Reflection spectroscopy is a useful method for the *in situ* characterization of the monolayer at the air-water interface,^[64, 65] providing relevant information about orientation of the molecules in the film, formation and types of aggregates, changes in the aggregation state upon the compression process, etc. However, it is

well-known that the normalized reflection spectra, $\Delta R_n = \Delta R \cdot A$ of the films provide more direct information about the orientation of the molecules upon the compression process since the influence of the surface density is eliminated.^[65, 66] Normalized reflection UV-vis spectra, ΔR_n , recorded at different surface pressures for OPE2A Langmuir (L) films are shown in Figure 5a. In addition, a quantitative analysis of the ΔR_n spectra has allowed us to calculate the tilt angle of the transition dipole moment of the molecule with respect to the liquid surface, ϕ (Figure 5b). This angle was determined by comparing the reflection spectra at air-water interface and the UV-vis absorption spectrum of OPE2A in solution as has been comprehensively detailed elsewhere.^[61, 65] The tilt angle of the OPE moieties with respect to the water subphase is largely unchanged upon compression when the monolayers are prepared onto a water subphase and only a small variation in ΔR_n values is produced in the basic subphase. The tilt angle of the molecules is around 60° for films onto pure water subphase and slightly higher, ca. 67°, in the condensed phase of a monolayer onto the basic subphase, which is in agreement with the more expanded isotherm observed in pure water (Figure 5b).

Interestingly, the reflection band is shifted with respect to the solution depending on the subphase in which the monolayers are prepared. Within the last few years a systematic study in which different polar terminal groups have been added to the OPE skeleton as well as alkyl chains of different length or other hydrophobic terminal groups has been carried out. In all the previously studied cases,^[12, 14, 19, 20, 26, 58, 63, 67-70] hypsochromic shifts of the main absorption band with respect to the solution were observed both in Langmuir (L) and LB films, with this blue-shift of the films being attributed to the formation of H-aggregates. To our knowledge this is the first example of an OPE derivative which when arranged in a Langmuir film shows a bathochromic shift (monolayers onto pure water). However, the observation of a hypsochromic shift is maintained for monolayers onto a basic subphase. It is also worth of note that monosubstituted carboxylic acid OPE derivatives incorporated in L and LB films showed a significant hypsochromic shift (36-60 nm) compared to the solution spectrum,^[19, 26, 71] (with this shift being independent of the pH of the subphase) which leads to the conclusion that the effect observed in OPE2A is a unique feature of this dicarboxylic substituted compound. The red-shift of OPE2A in L films prepared onto water could be due to several factors:

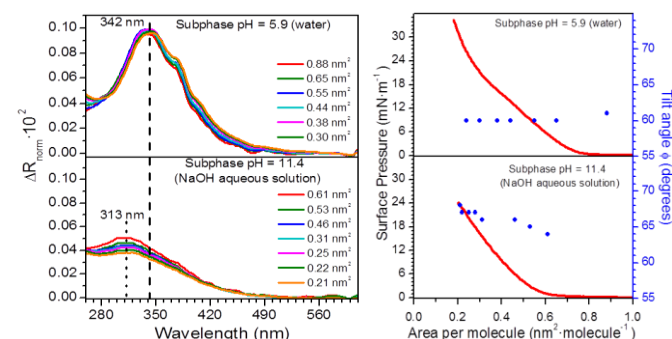


Figure 5. a) Normalized reflection spectra upon compression at the indicated surface pressures for OPE2A monolayers prepared onto the indicated subphases. b) Tilt angle (ϕ) of OPE2A with respect to the liquid surface upon the compression process for monolayers prepared onto the indicated subphases.

(i) *Solvatochromic effect*; in order to understand the influence of polarity in aggregation, OPE2A was dissolved in solvents from

CHCl₃ to EtOH/water mixtures (this compound is not soluble in apolar solvents). A significant hypsochromic-shift was observed, from 325 nm (CHCl₃) to 315 nm (EtOH) and 302 nm (EtOH/H₂O 2:1). This result indicates that the red-shift observed is not attributable to an increase in the environment polarity as might be expected at the air-water interface, especially at low surface pressures. However, due to the insolubility of this compound in apolar solvents it is not fully clear whether a less polar environment, which could be achieved in compact monolayers, might result in a red shift of the absorption profile.

- (ii) *Conjugation length*.^[72] It has been experimentally observed that OPE derivatives exhibit a red-shift when the number of phenylene-ethynylene groups increases. As will be demonstrated later, the OPE2A compound generates a supramolecular structure in monolayers through lateral hydrogen bond interactions when monolayers are fabricated onto a water subphase. These H-bonds could constrain the phenylene rings to adopt more planarized orientations, resulting in a more extended π -electron delocalization.^[73, 74]
- (iii) *Formation of J-aggregates*. It has been noted that for some compounds that tend to form mainly H-aggregates, e.g. merocyanines^[75, 76] and azo compounds,^[77, 78] the incorporation of certain functional groups capable of forming hydrogen bonds leads to the formation of J-aggregates, which exhibit absorption spectrum which are red-shifted with respect to the solution spectrum. However, taking into account the angle of OPE2A monolayers with respect to the surface, ca. 60° for monolayers spread onto pure water, and the angle needed, according to the theoretical calculations,^[79] to exhibit a red shift (<54°), we believe that although this effect could somehow contribute to the bathochromic effect might not be the main cause of the red shift observed for OPE2A Langmuir films.

The transfer of these Langmuir films onto solid supports gives Langmuir-Blodgett films, which can be investigated by a wider range of spectroscopic, microscopic, and electrochemical methods to provide further insight into the arrangement of OPE2A molecules in monolayers on different supports.

The transfer ratio calculated by the trough software during deposition of the monolayer was approximately 1 at a surface pressure of 20 mN·m⁻¹ for both pure water and aqueous NaOH subphases. This uniform transfer was also estimated using a quartz crystal microbalance (QCM). Thus, the frequency change (Δf) for a QCM quartz resonator before and after the deposition process was determined using the Sauerbrey equation:^[80]

$$\Delta f = - \frac{2 \cdot f_0^2 \cdot \Delta m}{A \cdot \rho_q^{1/2} \cdot \mu_q^{1/2}} \quad (1)$$

where f_0 is the fundamental resonant frequency of 5 MHz, Δm (g) is the mass change, A is the electrode area (cm²), ρ_q is the density of the quartz (2.65 g·cm⁻³), and μ_q is the shear module (2.95·10¹¹ dyn·cm⁻²). Considering these values and the OPE2A molecular weight (366 g·mol⁻¹), the surface coverages (Γ) obtained from Eq. 1 are 5.60·10⁻¹⁰ and 6.5·10⁻¹⁰ mol·cm⁻² for the water and basic

subphases, respectively. These values correspond to transfer ratios of 0.96 for the monolayer onto pure water and 0.98 for the monolayer onto a basic subphase.

Electrochemical electron transfer currents at electrodes under controlled potential provide an indirect measure of defect densities in thin films and can be conveniently studied by cyclic voltammetry for film coated electrodes.^[81, 82] Cyclic voltammograms (CVs) obtained from aqueous solutions containing 1 mM [Ru(NH₃)₆]Cl₃ and 0.1 M KCl for a bare gold and for a gold working electrode modified by an one layer LB film deposited at 5, 10, 15, and 20 mN·m⁻¹ from a monolayer prepared onto a pure water subphase are shown in Figure 6a (the same sort of sequence was obtained for monolayers prepared onto a basic subphase, not shown here for brevity). The electrochemical response of a bare gold electrode exhibits a clear voltammetric wave characteristic of the ruthenium complex. There is a significant decrease in current density for the voltammograms recorded using gold electrodes covered by the LB films, with this decrease in the current density being more significant as the surface pressure of transference increases. When the surface pressure of transference was 20 mN·m⁻¹, reduction and oxidation peaks of the redox probe for the modified electrode drastically decrease indicating effective blocking of the electrode surface and therefore a low density of holes or defects in the monolayer. In addition, LB films fabricated from a basic solution block the electrode slightly better than those prepared in pure water (see Figure 6b) in agreement with the results obtained by other techniques (e.g. a less expanded isotherm, a higher surface coverage, higher tilt angles, etc.)

As indicated in the introduction, self-assembly (SA) is a commonly used method to fabricate films incorporating functionalized OPEs. It is well-known that the LB method is not the most appropriate to assemble doubly polar functionalized molecules in which a strong competition of the polar groups to be anchored at the air-water interface could take place. However, in this particular case, the LB technique has shown itself as a good method to incorporate OPE2A molecules into well-ordered monolayers. This behaviour is probably due to the presence of a very rigid OPE backbone that prevents the molecule from bending and the two polar groups both contacting the water surface. In addition, the very hydrophobic OPE core tends to be situated away from the water surface leading to a surface behaviour similar to that of amphiphilic materials containing just one polar group. In order to compare the efficiency of the LB method with that of self-assembly (SA) in the arrangement of OPE2A molecules in terms of surface coverage, SAMs (self-assembled monomolecular films) of OPE2A were fabricated. Gold substrates were immersed for 48 hours in a 1.3·10⁻³ M solution of OPE2A in ethanol. The poor blocking of the gold electrode (Figure 6b) and a low coverage of OPE2A on gold surfaces was determined by QCM experiments (surface coverage of 3.8·10⁻¹⁰ mol·cm⁻² for SAMs which compares with 5.53·10⁻¹⁰ mol·cm⁻² for LB films prepared onto a water subphase).

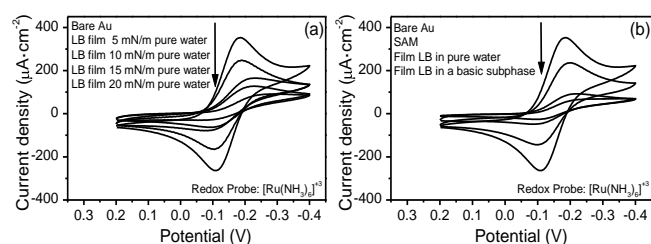


Figure 6. Cyclic voltammograms (CVs) of (a) a one-layer LB film of OPE2A (water subphase) deposited on a gold electrode at the indicated transference surface pressures. (b) Comparison of the blocking effect on the gold electrode of an LB film transferred at a surface pressure of 20 mN·m⁻¹ and a self-assembled film. CVs were recorded by immersing the gold substrate in a 1 mM [Ru(NH₃)₆]Cl₃ and 0.1 M KCl aqueous solution using a scan rate of 0.1 V·s⁻¹ at 20 °C. A Ag|AgCl saturated reference electrode was employed and the counter electrode was a Pt sheet.

Optical properties of the transferred films offer additional insight into the molecular arrangement and degree of order within the film. Langmuir films of OPE2A were transferred onto quartz substrates at 20 mN·m⁻¹ and the UV-vis absorption spectra were recorded. Figure 7 shows the electronic spectra of OPE2A LB films prepared from water and basic subphases together with the spectrum of OPE2A in solution and at the water-liquid interface for comparison purposes. Molar absorptivities for the monolayer and the solution were obtained according to the expressions:

Air-water interface:^[83]

$$\varepsilon = \frac{\Delta R}{2.303 \cdot 10^3 \cdot \Gamma \cdot \sqrt{R_w}} \quad (2)$$

Solution:

$$\varepsilon = \frac{A_b}{C \cdot \ell} \quad (3)$$

LB Films:

$$\varepsilon = \frac{A_b}{1000 \Gamma} \quad (4)$$

where Γ is the surface density given in mol·cm⁻², R_w is the water reflectivity (0.02), A_b is the absorbance, C is the solution concentration, and ℓ is the cell width.

The LB film spectrum of LB films transferred from a water subphase is again red-shifted by ca. 17 nm compared to the solution spectrum (see Figure 7), and practically overlaps with the spectrum of the monolayers at the air-water interface (result not shown for clarity). In the case of films transferred from a basic substrate the spectrum is blue shifted by 14 nm with respect to the solution and again the LB film spectrum overlaps the reflection spectrum obtained on a basic subphase. These results indicate that the molecular arrangement at the air-liquid interface is retained when the films are transferred onto the solid support. Additionally, the difference in the apparent molar absorptivity of the molecule in solution and within the films provides quantitative information of the orientation of the dipole moment of transition and the normal to the surface as stated before. The results here obtained clearly indicate that OPE2A molecules are in a more vertical orientation with respect to the substrate when they are fabricated from a basic subphase compared to those fabricated from a water subphase. LB films that were prepared using a water subphase were incubated during 48 h in a NaOH solution (pH = 11.4) after which were thoroughly rinsed with water and dry. The maximum wavelength is then shifted to 324 nm, i.e., the initial red-shift with respect to the solution disappears. This result is consistent with the red-shift in films prepared onto pure water being due to the presence of lateral H-bonds between neighbouring molecules that disappear after exposition of the film to a basic media. The fact that after incubation of these films in a water subphase the peak is not shifted to 313 nm (position of the maximum wavelength for films prepared onto a

basic subphase) may be attributable to a different orientation of the molecules in both films.

328	317	313	345
-----	-----	-----	-----

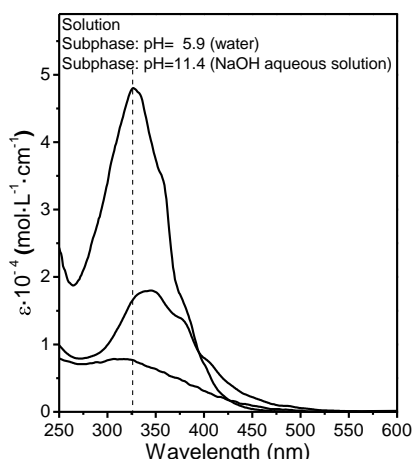


Figure 7. Molar absorptivity vs. wavelength for a monomolecular LB film of OPE2A transferred at $20 \text{ mN}\cdot\text{m}^{-1}$ from a water and basic subphase as indicated in the figure labels and in a $\text{CHCl}_3:\text{EtOH}$ 4:1 solution.

Table I shows additional evidence for the formation of a supramolecular structure within the L and the LB films. While the absorption maxima of L and LB films formed on an aqueous subphase ($\text{pH}=5.9$), where the carboxylic groups are expected to be protonated, is red-shifted with respect to the solution spectrum in chloroform, the peaks of L and LB films prepared onto a basic subphase (NaOH) are slightly blue-shifted. In basic subphases the carboxylic groups are deprotonated and therefore no H-bonds between adjacent molecules are formed. In addition, it seems that the red shift observed for the LB films onto the water subphase may be favoured by the spatial organization of the film since the maximum absorption for cast films of this compound prepared from a chloroform solution appears at 317 nm, i.e., again blue-shifted with respect to the solution (328 nm). A LB film fabricated using pure water in the subphase was redissolved in chloroform. A significant blue shift (peak at 300 nm) of the solution compared to the spectrum of the solution was observed. After sonication of the solution of the redissolved film in chloroform for 10 min minutes the original spectrum of this compound in a chloroform solution was obtained. This phenomenon indicates that no chemical reaction has taken place but definitely significant aggregation effects occur in the monolayer. The initial blue-shift of the spectrum after redissolving the film prepared from a water subphase might be due to the rupture of hydrogen bonds between neighbouring molecules and the preservation of lateral π - π interactions that may lead to H-aggregates. These interactions are lost after sonication. The electrical properties of the LB films also seem to point towards a different structure for films transferred from a water and a basic subphase (vide infra).

Table I. Position of the main absorption peak, expressed in nm, for the indicated solution and films.

Solution (CHCl_3)	Cast Film	LB film	
		Basic subphase $\text{pH} = 11.4$	Water subphase $\text{pH} = 5.9$

Carboxylic acids readily form head to head dimers in solution and solid state through mutual hydrogen bonding, which provides an avenue through which to explore the nature of the carboxylic acid groups in films of OPE2A, and to gather further support for the notion of a supramolecular network linking the exposed $-\text{CO}_2\text{H}$ moieties in LB films of this compound. Monolayers of OPE2A prepared onto the two subphases were transferred onto QCM substrates by withdrawal of the substrates that were initially immersed in the subphase. The modified substrates were introduced into a behenic acid solution (see Figure 8) and the frequency change (Δf) of the QCM quartz resonator before and after the exposure of monomolecular OPE2A films to a behenic acid solution was determined ($\text{CH}_3-(\text{CH}_2)_{20}-\text{COOH} \cdot 10^{-2} \text{ M}$ in CHCl_3). No frequency change was observed after 24 h incubation of the films transferred from a water subphase in the behenic acid solution. In contrast, after 4 hours of incubation of OPE2A films transferred from a basic subphase a frequency change of -27 Hz was recorded, which indicates, through application of the Sauerbrey equation, that one molecule of behenic acid has been deposited per molecule of OPE2A in the film. This result suggests that when OPE2A molecules are transferred from a water subphase the carboxylic acid remains protonated and lateral hydrogen bonds are formed which renders the $-\text{CO}_2\text{H}$ group insensitive to further H-bonding interactions. These hydrogen bonds are strong enough to prevent surface binding of behenic acid to the OPE2A monolayer through direct hydrogen bonding. However, when OPE2A molecules are transferred from a basic subphase the carboxylic acid groups are deprotonated and consequently they are free to form face to face hydrogen bonds with behenic acid molecules (see Figure 8). Although this QCM experiment clearly shows a different nature in the state of the terminal carboxylic groups, depending on the subphase used, it does not provide information about the dissociation state of the carboxylic groups directly attached to the gold substrate.

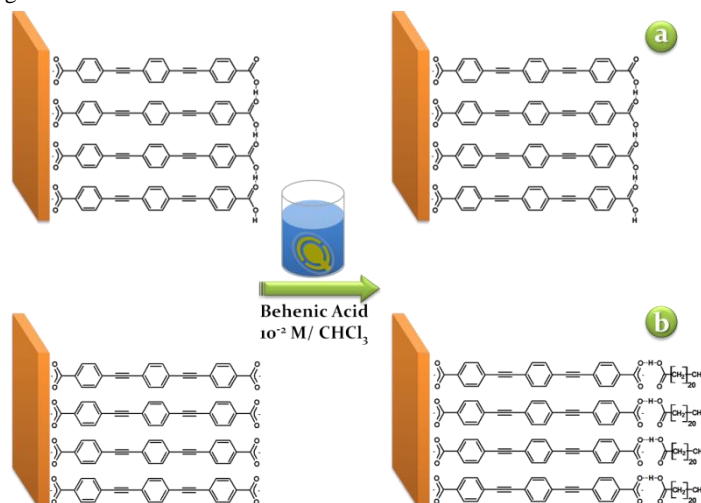


Figure 8. Scheme of monomolecular LB films deposited onto gold substrates and transferred from a water subphase (a) and a basic subphase (b) before and after incubation in a behenic acid solution according to the Quartz Crystal Microbalance experiments described in the text.

Figure 9 shows the XPS spectrum of the OPE2A powder as well as the spectra of OPE2A LB films transferred onto gold substrates from

the two different subphases, in the C1s spectral region. The powder spectrum shows a peak at 288.8 eV corresponding to the carbon atom in the carboxylic (-COOH) moiety.^[84-90] Films of OPE2A molecules on gold substrates prepared from a basic subphase result in a peak attributable to the carboxylate carbon at 287.1 eV.^[91, 92] This clearly indicates that OPE2A is entirely deprotonated when transferred from a basic subphase. In contrast, the peak at 288.8 eV is preserved in LB films transferred from a water subphase with the peak at 287.1 eV being also observed. This result indicates that OPE2A contains both carboxylate and carboxylic groups when transferred from a water subphase, which, in combination with the data provided by the QCM experiments above described, suggests that the group attached to the gold substrate is deprotonated and chemisorbed as carboxylate, independently of the subphase used. In contrast, the other terminal carboxylic group remains protonated when the Langmuir film is prepared onto a pure water subphase and is deprotonated when a basic subphase is used. Further confirmation of these conclusions was provided by angle-resolved X-ray Photoelectron Spectroscopy (AR-XPS). Representative C1s XPS spectra measured at two different take-off angles of 90° and 60° with respect to the surface are shown in Figure 10 for an OPE2A LB film prepared from pure water. From the AR-XPS spectra, it is clear that the intensity of the peak corresponding to the protonated carboxylic acid group, C_{COOH}, is larger while a decrease in the take-off angle results in a more prominent C_{COO⁻} peak. This result is consistent with the model presented in Figure 8 in which the adsorbate group contacting the gold surface is likely to be the deprotonated carboxylic acid group while the terminal carboxylic acid remains protonated.

The electrical behaviour of these two types of films, i.e. LB films of OPE2A transferred from a pure water subphase and a basic subphase, was studied showing very significant differences that may also be explained by the different protonation state of the carboxylic groups in these films.

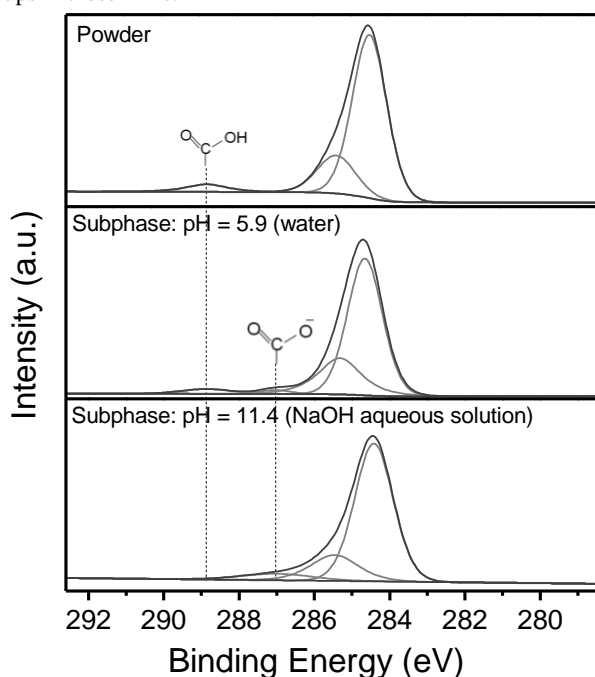


Figure 9. XPS spectra of C1s photoelectrons of OPE2A in powder and in LB films deposited onto gold substrates from a water and a basic aqueous subphase.

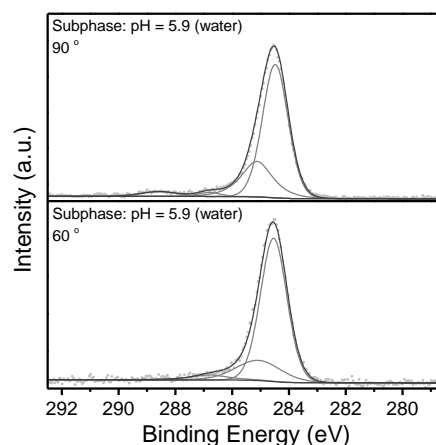


Figure 10. Angle resolved X-ray Photoelectron Spectra of a monomolecular LB film deposited onto a gold substrate from a pure water subphase using two different take-off angles, 90° and 60°.

To determine the electrical characteristics of a monomolecular LB film transferred onto gold substrates at 20 mN·m⁻¹ using pure water as subphase, *I-V* curves were recorded using a STM and averaged from multiple (ca. 420) scans at different locations on the substrate and using different samples to ensure the reproducibility and reliability of the measurements. Moreover, before recording the *I-V* curves, both the thickness of the monolayer and the tip-substrate distance (*s*) should be estimated in order to position the STM tip just above the LB film and, thus, avoid either penetration of the STM tip into the film or the existence of a substantial gap between the STM tip and the monolayer. Using the attenuation of the Au4f signal from the substrate - as explained in the experimental section - the thickness of the LB films on the gold electrode was estimated to be (1.81 ± 0.05) nm, in good agreement with the determination of the tilt angle obtained from the UV-vis reflection spectra at the air-water interface. Once the thickness of the LB film is known, calibration of the tip-substrate distance is needed so that the STM tip can be placed at a known distance above the LB film. This estimation is achieved by converting the set-point parameters of the STM (*I*₀ ≡ “set-point current” and *U*_t ≡ “tip bias”) to an absolute gap separation, as has been reported previously.^[93-95] To provide a reliable calibration of the tip-substrate distance, several *I(s)* scans were recorded during the experiment, that is, with the LB film adsorbed on the substrate and using a set point current of 20 nA, this means, the tip was in the LB film. *I(s)* scans used for this calibration did not show signs of wire formation (exponential decay of the current with the distance, without the presence of plateaux in the curve). Linear regression was used to determine the slope of ln(*I*) versus *s* in the *I* range that was relevant to the experiment. In this case, the average slope of the corresponding dln(*I*)/*ds* curves used to calculate the tip-substrate distance was 6.91 ± 1.37 nm⁻¹. This value is in good agreement with those reported for similar highly conjugated compounds incorporated in molecular films^[20, 26, 58] or for single molecules.^[21, 93] Using *U*_t = 0.6 V and *I*₀ = 0.15 nA as the set-point parameters, the initial tip-substrate distance is estimated as 1.82 nm according to equation 5. This value corresponds to the thickness of the monolayer. Therefore, using these set-point parameters the tip is positioned just above the monolayer. Meanwhile for higher set-point currents (for example, 0.6 nA (*s* = 1.63 nm)) the tip would be embedded within the monolayer and for lower set-point currents, the

tip would not be in contact with the monolayer and, in this case, the tunneling current measured represents tunneling through both the monolayer and the gap which exists between the top of the monolayer and the tip. Figure 11.a shows a representative I - V curve obtained for a one layer LB film using water as subphase at $U_t = 0.6$ V and $I_0 = 0.15$ nA. The profile of the I - V curve is clearly symmetrical and exhibits an approximately sigmoidal profile over the full voltage region. Nevertheless, the I - V curve becomes linear in the low voltage region (from -0.6 to +0.6 V), the ohmic region, where the conductance value is $0.26 \cdot 10^{-5} G_0$. This conductance value is significantly lower than other OPE derivatives assembled by the LB technique even when these OPE derivatives have different end groups.^[20, 26] This decrease in the conductance could be attributed to the presence of the carboxylic acid group that is used as linker to make the contact with the STM tip. Carboxylic acid groups promote a “supramolecular structure” within monolayers through lateral hydrogen bond interactions, which may also be synergistic with lateral π - π stacking. The lower conductivity for the carboxylic acid termination would then arise from the less effective contacting of this group to the gold STM tip when compared with the chemisorption bond formed between the carboxylate group and gold contacts.

A basic subphase (pH=11.4) was used to retain the under contacting group in its deprotonated carboxylate state. The thickness of the monolayer determined using the attenuation of the Au4f signal from the substrate was 1.95 ± 0.05 nm. Taking into account that the average slope of the corresponding $\ln(I)/ds$ curves used to calculate the tip-substrate distance was 5.48 ± 0.89 nm⁻¹ using the set-point parameters $U_t = 0.6$ V and $I_0 = 1$ nA, the initial tip-substrate distance is 1.95 nm, which is in agreement with the thickness of the monolayer indicating that the tip is positioned just above the monolayer when these set-point parameters are used. Figure 11.b shows a representative I - V curve obtained for a one layer LB film using a basic subphase at $U_t = 0.6$ V and $I_0 = 1$ nA. The profile of the I - V curve is clearly symmetrical and exhibits an approximately sigmoidal profile over the full voltage region, although the I - V curve becomes linear in the low voltage region (from -0.6 to +0.6 V), the ohmic region, where the conductance value is $1.75 \cdot 10^{-5} G_0$. This conductance value is similar or even larger than the conductance value obtained for other OPE derivatives assembled using the LB technique^[20, 58] or for single molecules.^[21, 93] In addition, Figure 11.b also shows an I - V curve constructed from single molecule conductance (SMC) values for OPE2A obtained by using the $I(s)$ method at eight different bias voltage values. This $I(s)$ method developed by Haiss et al.^[15, 21, 96] has been used to determine the single-molecule conductance of molecular junctions. The SMC-curve coincides with the I - V curve obtained for the LB film at 1 nA and 0.6 V indicating that with these parameters the STM tip is located directly above the LB film and electronically coupled to a single molecule. Both I - V curves show a similarity, despite the different molecular surroundings in the two cases: in the LB film the molecules are packed together with neighbouring OPE2A molecules, whereas no such neighbours exist for the SMC determinations. The higher conductance for the COO-Au molecular junctions than COOH-Au junctions, supports the notion that the former are more effective in both their surface binding ability and in promoting electrical transmission of the junctions, which is in agreement with previous work.^[38]

The sigmoidal shape of both I - V curves (using water or a basic subphase) is indicative of a non-resonant tunneling mechanism of transport through these metal-molecule-metal junctions. The Simmons model^[97] is one of the simplest tunneling barrier models which has been widely used for describing charge transport through metal | SAM or metal | LB film junctions.^[20, 56, 58, 98] In this model, the current I is defined as:

$$I = \frac{Ae}{4\pi^2 \hbar s^2} \left\{ \left(\Phi - \frac{eV}{2} \right) \exp \left[-\frac{2\sqrt{m}}{\hbar} \alpha \left(\Phi - \frac{eV}{2} \right)^{1/2} s \right] - \left(\Phi + \frac{eV}{2} \right) \exp \left[-\frac{2\sqrt{m}}{\hbar} \alpha \left(\Phi + \frac{eV}{2} \right)^{1/2} s \right] \right\} \quad (6)$$

for which V is the applied potential, A is the contact area of the molecule with the gold surface (0.31 nm² and 0.25 nm² for a water subphase or basic subphase, respectively in concordance with the isotherms shown in Figure 3 at the surface pressure of 20 mN·m⁻¹), s is the width of the tunneling barrier, which was assumed to be the through-bond distance between the end groups in OPE molecular wire as calculated with a molecular modeling program (2.07 nm), Φ is the effective barrier height of the tunneling junction (relative to the Fermi level of the Au), α is related to the effective mass of the tunneling electron and m and e represent the mass and the charge of an electron. Φ and α are the parameters which are then used to best fit the I - V data in Figure 11. Good agreement between the data and the model are obtained for $\Phi = 1.1$ eV and $\alpha = 0.41$ when water is used as subphase and for $\Phi = 0.73$ eV and $\alpha = 0.34$ when a basic subphase is used. Firstly, it is worth emphasizing that Eq. 5, which is based on a very simple model of non-resonant tunneling, gives a reasonable description of our experimental I - V data, and it is therefore reasonable to assume that the mechanism of transport through these metal-molecule-metal junctions is non-resonant tunneling. Secondly, if we compare both Φ values we observe that they are different depending on the subphase used. Thus, for a basic subphase, $\Phi = 0.73$ eV which is in good agreement to the value obtained for similar OPE derivatives assembled by self-assembly^[56, 99] or by the LB technique.^[14, 19, 20, 26, 58] Meanwhile, when the subphase is water, the effective barrier height is $\Phi = 1.1$ eV, a higher value compared to the one obtained for a basic subphase and for other OPE derivatives.^[20, 56, 58, 99] Therefore, these results seem to indicate that the presence of protonated surface groups (-COOH) and consequent lateral hydrogen bonds within the monolayer decreases the conductance. This is attributed to a more compromised electrical contact between the STM tip and the carboxylic acid terminated surface.

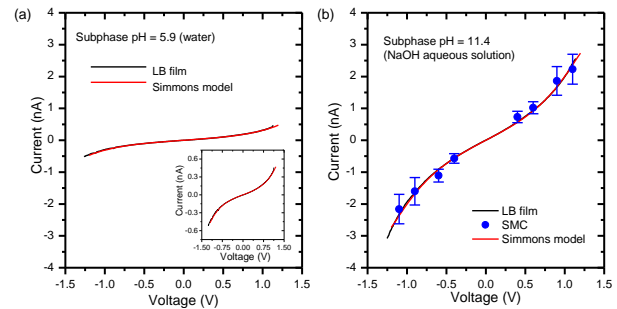


Figure 11. (a) I - V curve of a one layer LB film of OPE2A transferred onto Au(111) at 20 mN·m⁻¹ using as subphase water (black line) and fitting according to the Simmons equation, $\Phi = 1.1$ eV, $\alpha = 0.41$ (red line). The inset figure shows a magnification of the y-scale to observe in more detail the sigmoidal shape of the I - V graph. (b) I - V curve of a one layer LB film of OPE2A transferred onto Au(111) at 20 mN·m⁻¹ using a basic

subphase (black line), from single molecule conductance values obtained by using the $I(s)$ method (blue circles) and fitting according to the Simmons equation, $\Phi = 0.73$ eV, $\alpha = 0.34$ (red line). The error bars represent the standard deviation. $U_1 = 0.6$ V.

Conclusion

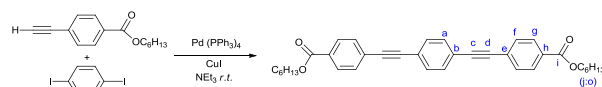
A symmetric acid terminal OPE derivative has been synthesized and assembled into well-packed monolayer films by means of the Langmuir–Blodgett technique which has shown itself as an adequate method for obtaining homogeneous films with a high surface coverage, which is better than those achieved by self-assembly technologies for this material. Langmuir films were prepared at the air–water interface using a pure water subphase and a basic subphase and characterized by surface pressure vs. area per molecule isotherms and Brewster angle microscopy, which revealed that OPE2A can form true monomolecular films at the air–water interface in both subphases in contrast to single acid substituted OPEs which only form three dimensional defect free monolayers on basic subphases. These monomolecular films were transferred undisturbed onto solid substrates with a transfer ratio close to 1. Both L and LB films of OPE2A fabricated onto a pure water subphase show a red-shift of the main absorption band with respect to the solution whilst films prepared onto a basic subphase exhibit a blue shift. A combination of QCM, XPS and UV-vis spectra experiments demonstrated that OPE2A was linked through a deprotonated carboxylic group to the gold substrate when the LB films are prepared from either a pure water or basic subphase. Monolayers fabricated onto a pure water subphase feature a supramolecular structure due to lateral H-bond interactions through the terminal carboxylic groups. In contrast, these lateral H-bonds are not present in monolayers fabricated onto basic subphases.

Electrical characteristics of the LB films on gold substrates were obtained by recording I - V curves with a gold STM tip positioned just above the monolayer (as determined from calibration of the tip-to-substrate distance and knowledge of the thickness of the LB film determined from XPS measurements). These I - V curves and good Simmons model fits indicate that charge flow through the OPE2A metal-molecule-metal junction is via a non-resonant tunnelling mechanism. Importantly, it is concluded that the conductance in films prepared onto basic subphases is quite similar to the SMC values. However, LB films fabricated onto a pure water subphase exhibit conductances around seven times lower. This result has been attributed to the more effective electrical junctions formed between carboxylate groups and gold surfaces, as compared to carboxylic acid groups which also form lateral H-bond interactions that decrease the conductance values. Thus, modulation of conductance by pH and molecular structure control is achieved.

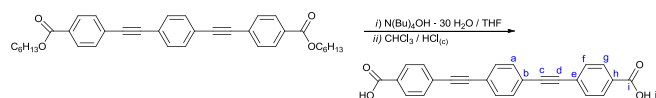
Experimental Section

General synthetic conditions

General conditions (syntheses) Synthetic reactions were carried out under an oxygen free nitrogen atmosphere using standard Schlenk techniques. All reaction vessels were flame-dried before use. Triethylamine was purified by distillation over CaSO_4 . Other reagents were purchased commercially and used as received. Compound hexyl-4-(ethynyl)benzoate was prepared according to literature procedures.^[26] NMR spectra were recorded in deuterated solvent solutions on Bruker DRX-400 and Varian 500 spectrometers and referenced against solvent resonances (^1H , ^{13}C). ESI mass spectra were recorded using a TQD mass spectrometer (Waters Ltd, UK). Samples were ($0.1 \text{ mg}\cdot\text{mL}^{-1}$) in analytical grade methanol. Thermal analyses were performed using a Perkin Elmer Pyris thermo-gravimetric analyser (heating rate $10 \text{ }^\circ\text{C}\cdot\text{min}^{-1}$).



Preparation of dihexyl 4,4'-(1,4-phenylenebis(ethyne-2,1-diyl))dibenzoate. To 25 mL Schlenk flask charged with NEt_3 (15 mL) with, hexyl-4-(ethynyl)benzoate (0.34 g, 1.5 mmol), 1,4-diodobenzene (0.25 g, 0.76 mmol), $\text{Pd}(\text{PPh}_3)_4$ (0.045 g, 0.040 mmol) and CuI (0.007 g, 0.037 mmol) were added and the resulting white suspension stirred at room temperature overnight. The precipitate was collected by filtration and washed thoroughly with hexane. The solids were dissolved in CH_2Cl_2 and filtered through silica gel. Solvent removal of the yellowish filtrate yielded the pure product as an off-white solid. Yield 0.30 g, 0.56 mmol, 75%. ^1H NMR (400 MHz, CDCl_3) δ 8.04 (d, $J = 9$ Hz, 4H, g), 7.59 (d, $J = 9$ Hz, 4H, f), 7.54 (s, 4H, a), 4.33 (t, $J = 7$ Hz, 2H, j), 1.82–1.72 (m, 4H, k), 1.49–1.40 (m, 4H, l), 1.39–1.29 (m, 8H, m/n), 0.92 (t, $J = 7$ Hz, 6H, o). ^{13}C NMR [^1H] (101 MHz, CDCl_3) δ 166.2 (i), 131.9, 131.6 (l/g), 130.3 (h), 129.7 (a), 127.6, 123.2 (b/e), 91.9, 90.9 (c/d), 65.5 (j), 31.6 (k), 28.8 (l), 25.8 (m), 22.7 (n), 14.1 (o). ASAP-MS(+) (ASAP) (m/z) 451.19 (100, $[\text{M}+\text{H}\cdot\text{C}_6\text{H}_{13}]^+$), 534.28 (53, $[\text{M}]^+$).



Preparation of 4,4'-(1,4-phenylenebis(ethyne-2,1-diyl))dibenzoic acid (OPE2A). To solution of dihexyl 4,4'-(1,4-phenylenebis(ethyne-2,1-diyl))dibenzoate (0.05 g, 0.09 mmol) in THF (3 mL), $\text{N}(\text{Bu})_4\text{OH}\cdot 30 \text{ H}_2\text{O}$ (0.30 g, 0.38 mmol) dissolved in THF (3 mL) was added. The resulting brown solution was stirred at room temperature for 30 minutes, taken to dryness and redissolved in CHCl_3 (2 mL). White solids precipitated upon addition of $\text{HCl}_{(aq)}$ and sonication of the two phases. The precipitate was collected by filtration and washed with water (2x5 mL), acetone (2 mL) and Et_2O (5 mL) and dried in air. Yield 0.03 g, 0.08 mmol, 89%. ^1H NMR (500 MHz, $\text{DMSO}-d_6$) δ 13.21 (br. s, 2H, j), 7.97 (d, $J = 8$ Hz, 4H, g), 7.67 (d, $J = 8$ Hz, 4H, f), 7.64 (s, 4H, a). ^{13}C NMR [^1H] (126 MHz, $\text{DMSO}-d_6$, $50 \text{ }^\circ\text{C}$) δ 166.4 (i), 131.6, 131.4 (l/g), 130.8 (h), 129.3 (a), 126.0, 122.2 (b/e), 91.1, 90.6 (c/d). ESI-MS(–) (m/z) 183.3 (100, $[\text{M}-2\text{H}]^-$), 365.5 (34, $[\text{M}-\text{H}]^-$). TGA shows incomplete combustion (91%) at $1000 \text{ }^\circ\text{C}$.

Film fabrication and characterization. The films were prepared on a Nima Teflon trough with dimensions $720 \times 100 \text{ mm}^2$, which was housed in a constant temperature ($20 \pm 1 \text{ }^\circ\text{C}$) cleaned room. A Wilhelmy paper plate pressure sensor was used to measure the surface pressure (π) of the monolayers. The sub-phase was Millipore Milli-Q, resistivity $18.2 \text{ M}\Omega\cdot\text{cm}$. To construct the Langmuir films a $1 \cdot 10^{-5} \text{ M}$ solution of OPE2A in chloroform:ethanol 4:1 (purchased from LabScan HPLC grade 99.8% and Panreac HPLC grade 99.5%, respectively) was spread using a Hamilton syringe held very close to the surface, allowing the surface pressure to return to a value close to zero between each addition. The use of ethanol (EtOH) in the spreading solvent serves to limit the formation of hydrogen-bonded carboxylic acid dimers and aggregates in solution prior to deposition.^[63] After waiting about fifteen minutes to allow the solvent to evaporate, slow compression of the film began at a speed of $0.022 \text{ nm}^2\cdot\text{molecule}^{-1}\cdot\text{min}^{-1}$. Under these experimental conditions the isotherms were highly reproducible. The direct visualization of the monolayer formation at the air/water interface was studied using a commercial micro-Brewster angle microscopy (micro-BAM) from KSV-NIMA, having a lateral resolution better than $12 \mu\text{m}$. An ultraviolet-visible (UV-vis) reflection spectrophotometer, with a light source FiberLight DTM 6/50 and an absolute wavelength accuracy $< 0.3 \text{ nm}$ and a resolution (Raylight-criterion) $> 3 \text{ nm}$, was used to obtain the reflection spectra of the Langmuir films during the compression process.^[65]

The monolayers at the air–water interface were transferred onto solid supports at a constant surface pressure by the vertical dipping method (dipping speed was $3 \text{ mm}\cdot\text{min}^{-1}$) onto gold or quartz substrates, which were carefully cleaned as described previously.^[100, 101] Quartz Crystal Microbalance (QCM) measurements were carried out using a Stanford Research Systems instrument and with AT-cut, α -quartz crystals with a resonant frequency of 5 MHz and circular gold electrodes patterned on both sides. UV-vis spectra of the LB films were acquired on a Varian Cary 50 spectrophotometer, and recorded using a normal incident angle with respect to the film plane.

Cyclic voltammetry (CV) experiments were carried out in an electrochemical cell containing three electrodes. The working electrode was made of a gold substrate modified by the deposited LB film, the counter electrode was a platinum sheet, and the reference electrode was $\text{Ag} | \text{AgCl} | \text{saturated KCl}$.

X-ray photoelectron spectroscopy (XPS) spectra were acquired on a Kratos AXIS ultra DLD spectrometer with a monochromatic Al $K\alpha$ X-ray source (1486.6 eV) using a pass energy of 20 eV. To provide a precise energy calibration, the XPS binding energies were referenced to the $\text{C}1s$ peak at 284.6 eV. The thickness of LB films on gold substrates was estimated using the attenuation of the $\text{Au}4f$ signal from the substrate according to $I_{\text{LB film}} = I_{\text{substrate}} \exp(-d/\lambda \sin\theta)$, where d is the film thickness, $I_{\text{LB film}}$ and $I_{\text{substrate}}$ are the average of the intensities of the $\text{Au}4f_{5/2}$ and $\text{Au}4f_{7/2}$ peaks attenuated by the LB film and from bare gold, respectively, θ is the photoelectron take-off angle, and λ is the effective attenuation length of the photoelectron ($4.2 \pm 0.1 \text{ nm}$).^[99] An Agilent STM running Picoscan 4.19 Software was used for the characterization of the electrical properties of the LB films. In these measurements the tip potential is

referred to as U_p . STM tips were freshly prepared for each experiment by etching of a 0.25 mm Au wire (99.99%) in a mixture of HCl (50%) and ethanol (50%) at +2.4 V. Gold films employed as substrates were purchased from Arrandee®, Schroerer, Germany. These were flame-annealed at approximately 800-1000 °C with a Bunsen burner immediately prior to use. This procedure is known to result in atomically flat Au(111) terraces.

Acknowledgements

L.M.B., S.M., and P.C. are grateful for financial assistance from Ministerio de Ciencia e Innovación from Spain and fondos FEDER in the framework of projects CTQ2009-13024 and MAT2010-10846-E. P.J.L. holds an EPSRC Leadership Fellowship. R.J.N. thanks EPSRC for funding. S.M. acknowledges his Ramón y Cajal position from Ministerio de Ciencia e Innovación (Spain). L.M.B and J.C. acknowledge their grants from Banco Santander and Ministerio de Economía y Competitividad.

References

- [1] A. Aviram, M. Ratner, *Chem. Phys. Lett.* **1974**, *29*, 277.
- [2] L. A. Bumm, J. J. Arnold, M. T. Cygan, T. D. Dunbar, T. P. Burgin, L. Jones II, D. L. Allara, J. M. Tour, P. S. Weiss, *Science* **1996**, *271*, 1705.
- [3] J. M. Tour, L. Jones II, D. L. Pearson, J. J. S. Lamba, T. P. Burgin, G. M. Whitesides, D. L. Allara, A. N. Parikh, S. V. Atre, *J. Am. Chem. Soc.* **1995**, *117*, 9529.
- [4] J. M. Beebe, V. B. Engelkes, L. L. Miller, C. D. Frisbie, *J. Am. Chem. Soc.* **2002**, *124*, 11268.
- [5] G. K. Ramachandran, T. J. Hopson, A. M. Rawlett, L. A. Nagahara, A. Primak, S. M. Lindsay, *Science* **2003**, *300*, 1413.
- [6] L. J. Richter, C. S.-C. Yang, P. T. Wilson, C. A. Hacker, R. D. van Zee, J. J. Stapleton, D. L. Allara, Y. Yao, J. M. Tour, *J. Phys. Chem. B* **2004**, *108*, 12547.
- [7] J. J. Stapleton, T. A. Daniel, S. Uppili, O. M. Carbarcos, J. Naciri, R. Shashidhar, D. L. Allara, *Langmuir* **2005**, *21*, 11061.
- [8] L. Venkataraman, J. E. Klare, I. W. Tam, C. Nuckolls, M. S. Hybertsen, M. N. Steigerwald, *Nano Lett.* **2006**, *6*, 458.
- [9] S. Yasuda, S. Yoshida, J. Sasaki, Y. Okutsu, T. Nakamura, A. Taninaka, O. Takeuchi, H. Shigekawa, *J. Am. Chem. Soc.* **2006**, *128*, 7746.
- [10] B. Kim, J. M. Beebe, Y. Jun, X. Y. Zhu, C. D. Frisbie, *J. Am. Chem. Soc.* **2006**, *128*, 4970.
- [11] D. Venkataraman, Y. S. Park, A. C. Whaley, C. Nuckolls, M. S. Hybertsen, M. L. Steigerwald, *Nano Lett.* **2007**, *7*, 502.
- [12] G. Pera, A. Villares, M. C. Lopez, P. Cea, D. P. Lydon, P. J. Low, *Chem. Mater.* **2007**, *19*, 857.
- [13] S. Martín, W. Haiss, S. J. Higgins, P. Cea, M. C. Lopez, R. J. Nichols, *J. Phys. Chem. C* **2008**, *112*, 3941.
- [14] A. Villares, D. P. Lydon, P. J. Low, B. J. Robinson, G. J. Ashwell, F. M. Royo, P. Cea, *Chem. Mater.* **2008**, *20*, 258.
- [15] C. Wang, A. S. Batsanov, M. R. Bryce, S. Martin, R. J. Nichols, S. J. Higgins, V. M. Garcia-Suarez, C. J. Lambert, *J. Am. Chem. Soc.* **2009**, *131*, 15647.
- [16] M. Kamenetska, M. Koentopp, A. C. Whalley, Y. S. Park, M. L. Steigerwald, C. Nuckolls, M. S. Hybertsen, L. Venkataraman, *Phys. Rev. Lett.* **2009**, *102*, 126803.
- [17] M. Paulsson, C. Krag, T. Frederiksen, M. Brandbyge, *Nano Lett.* **2009**, *9*, 117.
- [18] C. Ko, M. Huang, M. Fu, C. Chen, *J. Am. Chem. Soc.* **2010**, *132*, 756.
- [19] A. Villares, G. Pera, S. Martin, R. J. Nichols, D. P. Lydon, L. Applegarth, A. Beeby, P. J. Low, P. Cea, *Chem. Mater.* **2010**, *22*, 2041.
- [20] G. Pera, S. Martin, L. M. Ballesteros, A. J. Hope, P. J. Low, R. J. Nichols, P. Cea, *Chem. Eur. J.* **2010**, *16*, 13398.
- [21] S. Martin, I. Grace, M. R. Bryce, C. S. Wang, R. Jitchati, A. S. Batsanov, S. Higgins, C. J. Lambert, R. J. Nichols, *J. Am. Chem. Soc.* **2010**, *132*, 9157.
- [22] S. Martin, W. Haiss, S. J. Higgins, R. J. Nichols, *Nano Lett.* **2010**, *10*, 2019.
- [23] A. Mishchenko, L. A. Zotti, D. Conlanthen, M. Bulrkle, F. Pauly, J. C. Cuevas, M. Mayor, T. Wandlowski, *J. Am. Chem. Soc.* **2011**, *133*, 184.
- [24] B. Kim, S. H. Choi, X.-Z. Zhu, C. D. Frisbie, *J. Am. Chem. Soc.* **2011**, *133*, 19864.
- [25] Y. Kim, T. J. Hellmuth, M. Bulrkle, F. Pauly, E. Scheer, *ACS Nano* **2011**, *5*, 4104.
- [26] L. M. Ballesteros, S. Martin, M. C. Momblona, S. Marques-Gonzalez, M. C. Lopez, R. J. Nichols, P. J. Low, P. Cea, *J. Phys. Chem. B* **2012**, *116*, 9142.
- [27] D. Villaume, *Comptes Rendus Physique* **2008**, *9*, 78.
- [28] B. Mann, H. Kuhn, *J. Appl. Phys.* **1971**, *42*, 4398.
- [29] J. G. Kushmerick, D. B. Holt, J. C. Yang, J. Naciri, M. H. Moore, R. Shashidhar, *Phys. Rev. Lett.* **2002**, *89*, 086802.
- [30] H. Basch, R. Cohen, M. A. Ratner, *Nano Lett.* **2005**, *5*, 1668.
- [31] D. Venkataraman, J. E. Klare, C. Nuckolls, M. S. Hybertsen, M. L. Steigerwald, *Nature* **2006**, *442*, 904.
- [32] R. B. Pontes, A. R. Rocha, S. Sanvito, A. Fazzio, A. da Silva, J. Roque, *ACS Nano* **2011**, *5*, 795.
- [33] Y. Selzer, A. Salomon, D. Cahen, *J. Am. Chem. Soc.* **2002**, *124*, 2886.
- [34] F. Rissner, D. A. Egger, L. Romaner, G. Heimel, E. Zojer, *ACS Nano* **2010**, *4*, 6735.
- [35] H. P. Yoon, M. M. Maitani, O. M. Cabarcos, L. Cai, T. S. Mayer, D. L. Allara, *Nano Letters* **2010**, *10*, 2897.
- [36] S. N. Yaliraki, M. Kemp, M. A. Ratner, *J. Am. Chem. Soc.* **1999**, *121*, 3428.
- [37] Y. An, C. Yang, M. Wang, X. Ma, D. Wang, *J. Phys. Chem. C* **2009**, *113*, 15756.
- [38] F. Chen, X. Li, J. Hihath, Z. Huang, N. J. J. Tao, *J. Am. Chem. Soc.* **2006**, *128* (49), 15874.
- [39] W. Wang, L. Yu, *Langmuir* **2011**, *27*, 2084.
- [40] F. W. Del Rio, K. L. Steffens, C. Jaye, D. A. Fischer, R. F. Cook, *Langmuir* **2010**, *26*, 1688.
- [41] M. Kiguchi, H. Nakamura, Y. Takahashi, T. Takahashi, T. Ohto, *J. Phys. Chem. C* **2010**, 22254.
- [42] W. Haiss, C. S. Wang, R. Jitchati, I. Grace, S. Martin, A. S. Batsanov, S. J. Higgins, M. R. Bryce, C. J. Lambert, P. S. Jensen, R. J. Nichols, *Journal of Physics-Condensed Matter* **2008**, *20*, 374119.
- [43] S. Martin, D. Z. Manrique, V. M. Garcia-Suarez, W. Haiss, S. J. Higgins, C. J. Lambert, R. J. Nichols, *Nanotechnology* **2009**, *20*.
- [44] C. S. Wang, A. S. Batsanov, M. R. Bryce, S. Martin, R. J. Nichols, S. J. Higgins, V. M. Garcia-Suarez, C. J. Lambert, *Journal of the American Chemical Society* **2009**, *131*, 15647.
- [45] A. Nitzan, M. A. Ratner, *Science* **2003**, *300*, 1384.
- [46] N. J. Tao, *Nat. Nano* **2006**, *1*, 173.
- [47] R. E. Martin, F. Diederich, *Angew. Chem. Int. Ed.* **1999**, *38*, 1350.
- [48] U. H. F. Bunz, *Chem. Rev.* **2000**, *100*, 1605.
- [49] U. H. F. Bunz, *Acc. Chem. Res.* **2001**, *34*, 988.
- [50] F. R. F. Fan, J. P. Yang, L. T. Cai, D. W. Price, S. M. Dirk, D. V. Kosynkin, Y. X. Yao, A. M. Rawlett, J. M. Tour, A. J. Bard, *J. Am. Chem. Soc.* **2002**, *124*, 5550.
- [51] D. K. James, J. M. Tour, *Chem. Mater.* **2004**, *16*, 4423.
- [52] U. H. F. Bunz, *Adv. Polym. Sci.* **2005**, *177*, 1.
- [53] W. P. Hu, H. Nakashima, K. Furukawa, Y. Kashimura, K. Ajito, Y. Q. Liu, D. B. Zhu, K. Torimitsu, *J. Am. Chem. Soc.* **2005**, *127*, 2804.
- [54] D. K. James, J. M. Tour, *Top. Curr. Chem.* **2005**, *257*, 33.
- [55] X. Yin, H. M. Liu, J. W. Zhao, *J. Chem. Phys.* **2006**, *125*, 094711.
- [56] Q. Lu, K. Liu, H. Zhang, Z. Du, X. Wang, F. Wang, *ACS Nano* **2009**, *3*, 3861.
- [57] P. Kalinginedi, P. Moreno-Garcia, H. Valkenier, W. Hong, V. M. Garcia-Suarez, P. Buitter, J. L. H. Otten, J. C. Hummelen, C. J. Lambert, T. Wandlowski, *J. Am. Chem. Soc.* **2012**, *134*, 5262.
- [58] L. M. Ballesteros, S. Martín, G. Pera, P. A. Schauer, N. J. Kay, M. C. Lopez, P. J. Low, R. J. Nichols, P. Cea, *Langmuir* **2011**, *27*, 3600.
- [59] H. Kaji, Y. Shimoyama, *Jpn. J. Appl. Phys.* **2001**, *40*, 1396.
- [60] S. Martin, P. Cea, G. Pera, M. Haro, M. C. Lopez, *Journal of Colloid and Interface Science* **2007**, *308*, 239.
- [61] G. Pera, A. Villares, M. C. López, P. Cea, D. P. Lydon, P. J. Low, *Chem. Mater.* **2007**, *19*, 857.
- [62] M. Levitus, K. Schmieder, H. Ricks, K. D. Shimizu, U. H. F. Bunz, M. A. Garcia-Garibay, *J. Am. Chem. Soc.* **2001**, *123*, 4259.
- [63] A. Villares, D. P. Lydon, L. Porres, A. Beeby, P. J. Low, P. Cea, F. M. Royo, *J. Phys. Chem. B* **2007**, *111*, 7201.
- [64] J. M. Pedrosa, M. T. Martín, L. Camacho, D. Möbius, *J. Phys. Chem. B* **2002**, *106*, 2583.
- [65] P. Cea, S. Martín, A. Villares, D. Möbius, M. C. López, *J. Phys. Chem. B* **2006**, *110* 963.
- [66] M. Haro, J. del Barrio, A. Villares, L. Oriol, P. Cea, M. C. Lopez, *Langmuir* **2008**, *24*, 10196.
- [67] Z. X. Tang, R. K. Hicks, R. J. Magyar, S. Tretiak, Y. Gao, H. L. Wang, *Langmuir* **2006**, *22*, 8813.
- [68] A. Villares, D. P. Lydon, B. J. Robinson, G. J. Ashwell, F. M. Royo, P. J. Low, P. Cea, *Surface Science* **2008**, *602*, 3683.
- [69] A. Villares, S. Martin, I. Giner, J. Diaz, D. P. Lydon, P. J. Low, P. Cea, *Soft Matter* **2008**, *4*, 1508.
- [70] A. Villares, G. Pera, D. P. Lydon, M. C. Lopez, P. J. Low, P. Cea, *Colloid Surface A* **2009**, *346*, 170.
- [71] A. Villares, D. P. Lydon, L. Porès, A. Beeby, P. J. Low, P. Cea, F. M. Royo, *J. Phys. Chem. B* **2007**, *111*, 7201.
- [72] X. Tang, T. W. Schneider, J. W. Walker, D. A. Buttry, *Langmuir* **1996**, *12*, 5921.
- [73] W. Hu, N. Zhu, W. Tang, D. Zhao, *Org. Lett.* **2008**, *10*, 2669.
- [74] W. Hu, Q. Yan, D. Zhao, *Chem. Eur. J.* **2011**, *17*, 7087.
- [75] K. Ikegami, *Current Applied Physics* **2006**, *6*, 813.
- [76] Y. Hirano, Y. Tokuoka, N. Kawashima, Y. Ozaki, *Vibrational Spectroscopy* **2007**, *43*, 86.
- [77] C. Ouyang, S. Chen, B. Che, G. Xue, *Colloids. Surf. Physicochem. Eng. Aspects.* **2007**, *301*, 346.
- [78] K. K. Karukstis, L. A. Perelman, W. K. Wong, *Langmuir* **2002**, *18*, 10363.
- [79] D. C. Barber, R. A. Freitag-Beeston, D. G. Whitten, *J. Phys. Chem.* **1991**, *95*, 4074.
- [80] G. Sauerbrey, *Z. Physik* **1959**, *155*, 206.
- [81] M. D. Porter, T. B. Bright, D. L. Allara, C. E. D. Chidsey, *J. Am. Chem. Soc.* **1987**, *109*, 3559.
- [82] P. Cea, M. C. Lopez, S. Martin, A. Villares, G. Pera, I. Giner, *J. Chem. Edu.* **2009**, *86*, 723.
- [83] H. Grüniger, D. Möbius, H. Meyer, *J. Chem. Phys.* **1983**, *79*, 3701.

- [84] J. F. Moulder, W. F. Stickle, P. E. Sobol, K. D. Bomben, *Handbook of X-ray Photoelectron Spectroscopy*, MN, **1992**.
- [85] T. L. Marshbanks, H. K. Jugduth, D. W. N., E. I. Franses, *Thin Solid Films* **1993**, 232, 126.
- [86] E. Frydman, H. Cohen, R. Maoz, J. Sagiv, *Langmuir* **1997**, 13, 5089.
- [87] P. Allongue, M. Delamar, B. Desbat, O. Fagebaume, R. Hitmi, J. Pinson, J.-M. Saveant, *J. Am. Chem. Soc.* **1997**, 201.
- [88] M. R. Alexander, S. Payan, T. Duc, *Surf. Interface Anal.* **1998**, 26, 961.
- [89] S. W. Han, S. W. Joo, T. H. Ha, Y. Kim, K. Kim, *J. Phys. Chem. B.* **2000**, 104, 11987.
- [90] A. Adenier, M.-C. Bernard, M. M. Chehimi, E. Cabet-Deliry, B. Desbat, O. Fagebaume, J. Pinson, F. Podvorica, *J. Am. Chem. Soc.* **2001**, 123, 4541.
- [91] L. Pranger, A. Goldstein, R. Tannenbaum, *Langmuir* **2005**, 21, 5396.
- [92] G. Liu, J. Liu, T. Böcking, P. K. Eggers, J. J. Gooding, *Chem. Phys.* **2005**, 319, 136.
- [93] W. Haiss, C. S. Wang, I. Grace, A. S. Batsanov, D. J. Schiffrin, S. J. Higgins, M. R. Bryce, C. J. Lambert, R. J. Nichols, *Nature Materials* **2006**, 5, 995.
- [94] W. Haiss, S. Martin, E. Leary, H. van Zalinge, S. J. Higgins, L. Bouffier, R. J. Nichols, *Journal of Physical Chemistry C* **2009**, 113, 5823.
- [95] G. Sedghi, K. Sawada, L. J. Esdaile, M. Hoffmann, H. L. Anderson, D. Bethell, W. Haiss, S. J. Higgins, R. J. Nichols, *J. Am. Chem. Soc.* **2008**, 130, 8582.
- [96] W. Haiss, H. van Zalinge, S. J. Higgins, D. Bethell, H. Höbenreich, D. J. Schiffrin, R. J. Nichols, *J. Am. Chem. Soc.* **2003**, 125, 15294.
- [97] J. G. Simmons, *J. Appl. Phys.* **1963**, 281, 1793.
- [98] H. B. Akkerman, R. C. G. Naber, B. Jongbloed, P. A. van Hal, P. W. M. Blom, D. M. de Leeuw, B. de Boer, *Proc. Natl. Acad. Sci. U.S.A.* **2007**, 104, 11161.
- [99] K. Liu, G. Li, X. Wang, F. Wang, *J. Phys. Chem. C* **2008**, 112, 4342.
- [100] S. Martín, P. Cea, C. Lafuente, F. M. Royo, M. C. López, *Surf. Sci.* **2004**, 563, 27.
- [101] P. Cea, C. Lafuente, J. S. Urieta, M. C. López, F. M. Royo, *Langmuir* **1996**, 12, 5881.

